

## Modeling the Disk in the $\epsilon$ Aurigae System: a Brief Review With Proposed Numerical Solutions

Richard L. Pearson, III

Robert E. Stencel

*University of Denver, Department of Physics and Astronomy, 2112 E. Wesley Avenue, Denver, CO 80208; address email correspondence to richard.pearson@du.edu*

*Received April 19, 2012; revised July 19, 2012; accepted August 7, 2012*

**Abstract** Parameters associated with the opaque disk in  $\epsilon$  Aurigae are explored in the context of circumstellar and proto-planetary disk theory. The observed blackbody temperatures of the disk, at 550 and 1150 K, are primarily discussed. Brief reviews of previous work are included that describe and attempt to explain this temperature gradient. Heating from only the central B star provides a basal temperature of about 250 K. An accretion rate (from the disk to the B star) of  $10^{-7} M_{\odot}/\text{yr}$  also provides a similar basal temperature; a rate of  $1.5 \times 10^{-5} M_{\odot}/\text{yr}$  produces temperatures greater than 3000 K in the disk plane. To include the F star contribution, Monte Carlo radiative transfer tools can be used to examine numerous separation distances between the two stellar components, with the goal of matching the observed and modeled temperatures. An estimation of the distance to  $\epsilon$  Aurigae can then be extracted. The proposed method is described here.

### 1. Introduction

$\epsilon$  Aurigae is a single-line spectroscopic binary that features an opaque disk around a companion that causes lengthy eclipses every 27 years (for a reading list, see Carroll *et al.* 1991; Lissauer *et al.* 1996; Stencel *et al.* 2011). Figure 1 illustrates the configuration. Interferometric imaging proves the existence of a disk and provides some preliminary dimensions for it (Kloppenborg *et al.* 2010), based on a highly uncertain Hipparcos distance of 625 pc (Perryman *et al.* 1997). The eclipse of 2010 provided a wealth of new data, from far-ultraviolet to far-infrared and sub-mm wavelengths (Hoard *et al.* 2010; Stencel *et al.* 2011; Hoard *et al.* 2012). For this work, we are specifically interested in the observed surface temperatures of the disk as stated in Hoard *et al.* (2012) and provided here in Table 1.

There is an unresolved concern in regards to pinpointing the evolutionary state of  $\epsilon$  Aur. Two parts of this concern deal with the stellar masses and the distance to the system. First, the masses are unknown, but the bright primary star resembles an F0 supergiant that may contain as much as 15–25  $M_{\odot}$ , or as little as 3–4  $M_{\odot}$  (if it is an overluminous post-AGB star, as in Guinan and Dewarf

2002). Little to no optical spectrum exists for the disk-shrouded companion and thus it cannot be classified directly. Spectroscopic information provides a mass function value of 2.53 (Stefanik *et al.* 2010) and admits distance-dependent mass ratios of 0.5–1.1. Eclipse data and ultraviolet fluxes suggest the hidden companion could be a  $\approx 6 M_{\odot}$  B5V star (Hoard *et al.* 2010), with the bright star an approximately  $3 M_{\odot}$  hyper-luminous post-AGB star in a rapid state of evolution (Lambert and Sawyer 1986; Takeuti 1986a; Saito *et al.* 1987; Sheffer and Lambert 1999).

Second, the actual distance to  $\epsilon$  Aur is not well defined. The system is at the limit of a valid Hipparcos parallactic distance. There also seems to be intrinsic variability in the F star, which provides a varying star photocenter for the parallactic measurements (Kloppenborg *et al.* 2011). Of course, an accurate distance measurement refines the constraints on the system's physical parameters (for example, stellar masses, star-to-disk separations, and so on). Some of the typical parameters, using the high-error Hipparcos distance, are listed in Table 1.

Previous analytical and numerical modeling techniques have focused on resolving the questionable state of  $\epsilon$  Aur, by understanding the disk to constrain certain parameters of the entire system. These include disk thickness limitations (Lissauer *et al.* 1996), disk temperature studies (Takeuti 1986b; Hoard *et al.* 2010; Takeuti 2011), and spectral energy distribution (SED) matching (Muthumariappan and Parthasarathy 2012), for example. Many of these models used the Hipparcos distance to define parameters and/or used only specific parts of the system in the modeling (that is, considering only the disk and B star).

In order to support the plethora of observations, modeling techniques must further explore the complete nature of this disk. The observed minimum and maximum disk temperatures ( $T_{\text{noon}} = 1150 \pm 50$  K and  $T_{\text{midnight}} = 550 \pm 50$  K) provide an avenue of investigation (Hoard *et al.* 2012). One can look to reproduce these temperatures in analytical and numerical studies, by examining four  $\epsilon$  Aur disk-heating scenarios:

1. radiation from the central star (section 2.1),
2. accretional heating from the disk onto the central star (section 2.2),
3. radiation from the central and companion stars (section 2.3), and
4. radiation from stars plus accretional heating (also section 2.3).

The motivation of this paper is to describe the need to build a complete model of the  $\epsilon$  Aur system by using numerical modeling techniques and the observed temperatures. From this, a distance can be determined (as described in section 2.3.2), thereby clarifying the evolutionary state. Sections 2.1 and 2.2 establish possible disk basal temperatures and clarify that the observed temperature gradient must be achieved by an external source. Section 2.3

describes how numerical modeling of all heating components can aid in system constraints. This paper presents a brief review of previous modeling techniques and proposes additional numerical solutions.

## 2. Disk heating

A very useful tool in constraining certain parameters of the system are the disk temperatures. By matching observationally constructed SEDs with blackbody temperature curves, two temperatures have been established (Hoard *et al.* 2012). Half of the disk facing opposite the F star is the “midnight” side and found to be  $550 \pm 50$  K. The side facing the F star, “noon,” is found to have a temperature of  $1150 \pm 50$  K. Deciphering how and why the disk exhibits the observed temperature gradient is important in understanding the actual state of the system.

We explore heating effects on the disk by three different sources: heating from the central star, accretional heating, and the exterior stellar source are all investigated below. Brief reviews of prior work are included as well.

### 2.1. Central star input

We first consider a discussion concerning the effect of the central star radiation on the surrounding disk. Takeuti (1986b) analytically solved for the temperature and scale height of the disk at specified radii, based on a central B star of  $4 M_{\odot}$ ,  $3 R_{\odot}$ , and  $T_{\text{eff}} = 15000$  K. Blackbody equilibrium temperatures of 355 and 263 K were found at disk radii of 2 and 3 AU, respectively. No numerical radiative transfer analysis was performed. The significance of these values is discussed below.

More recently, Muthumariappan and Parthasarathy (2012, hereafter M&P) investigated the composition, dust particle size, outer radius temperature, and mass of the disk in  $\epsilon$  Aur, using a two-dimensional, photon-tracking Monte Carlo code. Their SED results were based on energy input only from an internal B5V star. The system was assumed to be at the Hipparcos distance. They created models with dust compositions of amorphous carbon, ISM distribution (60% silicates and 40% carbonates), and amorphous silicates. Also, particle size distributions corresponding to minima--maxima ranges of  $0.05\text{--}0.2 \mu\text{m}$  and  $10\text{--}100 \mu\text{m}$  were applied. A Kurucz flux model of a 7700 K, F0Iae post-AGB star was combined with the output SEDs. Then, comparisons were made with the observationally determined SED.

Their SED fitting resulted in a  $5 \times 10^{-3} M_{\odot}$  disk composed of carbonates, with grain sizes  $10\text{--}100 \mu\text{m}$ , and an outer disk temperature of 252 K at  $R_{\text{out}} = 3.8$  AU. The other models result in outer disk temperatures of 261–293 K. These are, obviously, lower than the either of the observed  $T_{\text{midnight}}$  or  $T_{\text{noon}}$ . Takeuti (1986b) determined a very comparable temperature, as stated above. Though M&P provide no discussion concerning this, these findings indicate

that models based solely on the interior B5V radiation provide a possible basal heating level which can be compared against observation. Further implications of this basal temperature are discussed in section 2.3.

## 2.2. Accretion input

We now explore the disk temperature, specifically  $T_{\text{midnight}}$ , based solely on accretional heating from the disk to the central star. Armitage (2010, specifically section 3.3 therein) describes a set of general disk equations describing accreting, Keplerian disk systems (for additional discussion, see Lin and Papaloizou 1985). Turbulent motion is used as the primary source of angular momentum transport within the disk; it is portrayed as a turbulent viscosity in Equation 1 of Table 2. The Shakura-Sunyaev  $\alpha$  parameter (Shakura and Sunyaev 1973) is used to define the disk's viscosity.

The equations displayed in Table 2 have been adopted from Armitage (2010) and applied to the  $\epsilon$  Aur disk. A previous iteration of this analytical calculation is found in Takeuti (1986b), who uses a form of Equations 5, 9, and 10 in Table 2 (along with a central B star as described in the first paragraph of section 2.1) to calculate temperatures and scale heights at various disk radii. Updated temperatures and scale heights, as well as additional parameters such as disk mass and density, are presented in Table 3.

If the central star mass ( $M_{\text{star}}$ ), accretion rate ( $\dot{M}$ ), and disk radius ( $r_{\text{disk}}$ ) are known, the equations in Table 2 depend only upon the mass absorption coefficient ( $\kappa$ ), the mean molecular weight ( $\mu$ ), and the viscosity parameter ( $\alpha$ ). Therefore, by defining these six terms, a full set of parameters describing the system can be output. The opacity temperature dependence ( $\kappa = \kappa_0 T$ ) and constant ( $\kappa = 5 \times 10^{-3} \text{ cm}^2 \text{ g}^{-1}$ ) were selected from Lin and Papaloizou (1985) and Pollack *et al.* (1985). A molecular weight of 1.5 was selected, which is low enough to admit that the disk has a high gas-to-dust ratio, but shows it is not completely made of hydrogen gas ( $\mu = 1$ ). Hartmann *et al.* (1998) determined  $\alpha = 0.01$  for T Tauri star disks and that has been adopted here. Accretion rates were obtained from Pequette *et al.* (2011a), who concludes that having a  $\dot{M} \neq 0$  was a possible way to reproduce comparable model SEDs to the observed. Pequette *et al.* (2011a) state that only a high accretion rate provides an appropriate UV-to-IR ratio. For the analytic calculations here, two typical accretion disk rates of  $10^{-6}$  and  $10^{-7} M_{\odot}/\text{yr}$  were used along with  $1.5 \times 10^{-5} M_{\odot}/\text{yr}$  from Pequette *et al.* (2011a, 2011b).

Once each of the input variables have been specified, all other parameters become uniquely determined. Selected output variables are displayed in Table 3. Of note, the  $10^{-6}$  and  $10^{-7}$  accretion rates produce disk masses ( $2.9\text{--}9.25 \times 10^{-3} M_{\odot}$ ) comparable to the mass predicted by M&P ( $5 \times 10^{-3} M_{\odot}$ ); the  $1.5 \times 10^{-5}$  accretion rate produces a disk mass about ten times that of M&P.

For disk thickness-to-radius ratio comparisons, an observed value of 0.08 is given in Table 1. This ratio was calculated from the angular measurements of the

observed thickness of the disk and its radius. Lissauer *et al.* (1996) shows plots of  $z/R_d$ , which is equivalent to  $Nh/R_{out}$  where  $N$  is an integer number of scale heights in a distance  $z$ . The analytical calculations in Table 3 show that for the highest accretion rate, none of the  $Nh/R_{out}$  values fall near 0.08. However, ratios from the  $10^{-6}$  and  $10^{-7}$  accretion rates are comparable. The  $10^{-6}$  rate allows for  $N=1$  or  $N=2$ , depending on the central star mass. The  $10^{-7}$  rate seems to prefer either  $N=2$  or  $N=3$ , which also coincides with the Lissauer *et al.* (1996) models.

If we assume a dust sublimation temperature of 1500 K, then the  $T_c$  values for the highest accretion rate are too large, especially if particles are supposed to be coalescing into protoplanetary objects. However, as seen in Figure 2, the only  $\dot{M}$  to output a  $T_{disk}$  near the observed midnight temperature is the  $1.5 \times 10^{-5} M_{\odot}/\text{yr}$  rate. If accretional heating was solely responsible for providing the observed 550 K “midnight” temperature, then the predicted disk mass from the high accretion rate must be discussed. The disk mass from Table 3 is  $41 \times 10^{-3} M_{\odot}$ , or 43 Jupiter masses, which is much larger than any previous prediction. Were the disk mass more along the lines of the M&P  $5 \times 10^{-3} M_{\odot}$ , the timescale for the disk would be about 330 years; since eclipse light curves of  $\epsilon$  Aur have shown fairly constant magnitude drops for almost 170 years, a timescale of only 330 years seems very unlikely. The existence of a mass transfer stream (from the F star to the disk), however, could extend the life of the disk. Nevertheless, the predicted mass, high  $T_c$  values, and large  $h/R_{out}$  ratios dismiss the likelihood of a high accretion rate present in  $\epsilon$  Aur. However, it does not dismiss the presence of a lower accretional rate.

Accretional heating alone is not able to support the observed temperature distribution (550–1150 K) on the disk. However, just as in section 2.1, the low  $T_{disk}$  output from the lower accretion rates may be able to provide a lower bound temperature for the disk in the  $\epsilon$  Aur system. The effect and relationship with the other heating mechanisms are discussed at the end of section 2.3.

### 2.3. Companion star input

The two previous sections have illustrated the importance of including the F0 star’s radiation in the modeling to explain the disk’s azimuthal temperature gradient. Though an examination of separate heating components can provide specific constraints (that is, a basal temperature), the next step is to include all of the components of the system. A brief review of previous work relating to the disk temperature is described to further justify the need for new numerical computations. The results of these new calculations will help provide an independent measurement of  $\epsilon$  Aur’s distance.

#### 2.3.1. Previous analytical studies

As previously mentioned, Takeuti (1986b) calculated disk temperatures and scale heights from two separate radiation sources. Putting them together, Takeuti (1986b) postulates a possible disk configuration: a cool, thin disk

near “midnight” and subject only to the central star’s radiation; a crescent-shaped, optically thick region dominated by the F star’s radiation; and a small, optically thin region, directly opposite the F star near the disk’s edge. Using this configuration, a steady-state disk assumption, and a limiting  $T_{\text{midnight}} = 500$  K, an accretion rate of  $2 \times 10^{-11} M_{\odot}/\text{yr}$  is found. This accretion rate would not produce the observed UV excess (Hoard *et al.* 2010). Takeuti (1986b) outlines that further ultraviolet and infrared observations are needed to resolve the questions concerning the system.

Twenty-five years later, Takeuti (2011) performed some analytical calculations that explored the outer-edge disk temperature variation along the disk plane, as heated by F0 and B5V stars. The Hipparcos distance of 625 pc was used to generate linear separations in the system. It is noted that since the “noon” temperature is the average temperature of the F0-facing side of the disk—similar to the average “midnight” temperature over the half of the disk facing away from the F0 star—the maximum temperature at “noon” will be slightly greater than the average value,  $T_{\text{noon}}$  (see Figures 1 and 2, as well as Table 2 in Takeuti 2011). Exploratory calculations consisting of physically descriptive heat capacities provided variable temperatures around the disk. However, the implications (composition, particle size, and so on) of the heat capacities chosen were not considered. A maximum temperature of 1200 K provided an upper limit for the calculations. Temperatures at the “midnight” position were found to be 250, 500, and 750 K. Scale heights were also calculated to provide an additional physical correlation with prescribed models. Accretional heating was ignored during this calculation. The work of Takeuti (2011) provides helpful constraints that can be used in numerical model calculations.

### 2.3.2. Proposed numerical analysis

The processing power and speed of current computers allow numerical simulations to effectively demonstrate physical configurations of astronomical systems quickly. For  $\epsilon$  Aur, using a three-dimensional (3D), photon-tracking Monte Carlo code will permit an inspection of disk temperatures according to radiation from both stellar components, as well as accretional heating. However, the unknown (or rather, the known but highly uncertain) distance creates significant problems in analyzing the radiation effects on the disk. Therefore, a distance— independent of any observations other than temperature—can be determined, based on the reproduction of the known temperatures,  $T_{\text{noon}}$  and  $T_{\text{midnight}}$  on the disk.

Figure 3 displays the process by which a distance can be determined. First, a distance ( $d^{\text{Model}}$ ) is selected. Then,  $d^{\text{Model}}$  is used to convert all of the well-determined angular separations into linear measurements. These parameters are then input into the Monte Carlo code. Next, the Monte Carlo code outputs a dust temperature file (described as “Disk Temperatures” in the figure). The points along the outer edge of the disk facing the F star, will be averaged— $\langle T_{\text{noon}}^{\text{Model}} \rangle$ —

and compared with  $\langle T_{\text{noon}}^{\text{Observed}} \rangle$ . If the modeled temperatures do not equal the observed, another distance is chosen and the process is continued. However, if the temperatures are equivalent, then the system can be defined by the chosen distance and additional parameters are calculated.

There will be an inherent range of distances that are capable of matching the averaged “noon” temperature, due to the observed temperature having an associated error of  $\pm 50$  K. However, the distance ranges should be sufficiently small to provide conclusive results. Once the distance has been established (with a certain amount of uncertainty), further systems parameters can be finalized: the mass function, the mass ratio, the two stellar masses, and the stellar radii. Knowing these, the evolutionary state of the system can be clarified.

Another feature that can be explored is the disk’s cooling (and heating) rate. However, the numerical modeling only provides a temperature snapshot of the “stable” system. No rotation of the disk is accounted for, and hence, the dust distributed in the disk has no prior incident heat or radiation. Therefore, the output temperatures only account for the snapshot of heating the dust receives at the specific moment being examined; a temperature distribution will still be present along the outer ridge of the disk (for example,  $T_{\text{noon}} > T_{\text{midnight}}$ ), due to shielding effects of the flared disk and the increased distance from the F star radiation. A temperature profile of the disk can be constructed (see Figure 4 for an example) and examined.

Comparisons of the snapshot temperature profile can be compared against a profile of a rotating disk. If a disk rotation is assumed, the dust particles directly in line with the companion F star, at “noon,” will heat up to some temperature,  $T_{\text{noon}}$ . As the disk’s dust rotates, the amount of radiation from the F star decreases; this allows the dust to begin its cooling process. The dust begins to heat up again when it again receives the F star radiation (see Takeuti 2011). The rate at which the heating and cooling occurs is highly dependent on the composition of the dust. Once the maximum and minimum temperatures are acquired in the numerical process outlined above, temperature-time profiles can be created following Takeuti (2011). Various disk compositions will result in various temperature-time profiles. The shape and slope of profile can be compared with the snapshot temperature profiles to assess the compatibility of the two.

There are a few other input parameters that will need to be fully explored. For instance, the accretion rate. Since it is an unknown, numerous iterations with various values of  $\dot{M}$  will need to be compared at each chosen distance. Limitations have been placed on  $\dot{M}$  previously, but since this is the first complete 3D numerical analysis of the whole system, a full range of accretional rates will be explored. Another required input is the density, composition, and particle size distribution of the disk. These aspects have a large impact on how the disk material interacts with the various heating sources and how it cools. Each will be explored with the technique described above. A complete set of solutions are forthcoming.

Currently, two 3D Monte Carlo codes are available that permit the inclusion of external radiation sources: Dullemond (2012) describes RADMC-3D, which uses a combination of FORTRAN and IDL packages; HYPERION is outlined in Robitaille (2011), using FORTRAN and PYTHON to complete its analysis. Both have the ability to model non-symmetric systems, which illustrates the power of 3D modeling.

### 2.3.3. A simple example of a 3D numerical calculation

To demonstrate the primary results from this 3D method, a hypothetical example is described here. Following the prescribed outline in Figure 3, an arbitrary distance of 830 pc was chosen. This places a user-defined F0 star (7750 K,  $150R_{\odot}$ ,  $3M_{\odot}$ ) about 30 AU from a disk-enveloped B5V star (15000 K,  $4R_{\odot}$ ,  $6M_{\odot}$ ) in RADMC-3D. A silicate disk was modeled with inner and outer radii of 1 and 4 AU. Only 10000 photon packets were launched during the radiative transfer calculation, creating a very statistically poor set of solutions; however, this is sufficient for this conjectured calculation.

The average disk-plane temperature at  $R_{\text{out}} = 4$  AU of the F0-facing disk was about 1500 K. This temperature is higher than the values predicted by Takeuti (2011) and  $\langle T_{\text{noon}}^{\text{Observed}} \rangle$ , but still relatively reasonable. The area of the disk at the “noon” position maxed at about 2500 K, which is significantly higher than the Takeuti (2011) estimation of about 1600 K. An average “midnight” temperature of about 900 K was found, which is also larger than the  $\langle T_{\text{midnight}}^{\text{Observed}} \rangle$ . A complete analysis, as described previously, is not presently provided. A graphical representation is shown in Figure 4.

It is noted that this brief example uses only a silicate disk and provides no accretional heating. A full analysis will examine the disk composition and will include an accretional rate. Still, the disregard for accretional heating may be a plausible assumption based on the B5V temperature: if the outward radiation pressure from the B5V star is large enough, it would severely limit the mass flow from the disk to the B5V star.

A final note is made here concerning the  $\langle T_{\text{midnight}}^{\text{Observed}} \rangle$  and the coldest temperature of the RADMC-3D model. A basal temperature of about 250 K was found in sections 2.1 and 2.2. The work by Takeuti (2011) place this basal temperature near the “dusk” position on the disk (refer to Figure 1). Therefore, one can expect the observed  $T_{\text{midnight}}$  to be larger than at “dusk.” However, in this hypothetical calculation, an average basal temperature was found at about 500 K. Adjustments to the distance, separation, composition, transmissivity, and/or other input parameters of the system can be made to find reasonable and comparable “dusk,” “noon,” and “midnight” temperatures.

Though just a hypothetical numerical calculation, this example shows that the temperature results will be able to provide distance and disk composition predictions. It outlines the usefulness of incorporating both stars in a numerical simulation and the need to explore the effects of accretional heating.

### 3. Conclusion

We have demonstrated the need for future analytical and numerical models of  $\epsilon$  Aur to include the radiation effects of the companion star. Additionally, we have proposed a way to determine the distance to the system by using the observed temperatures. A brief review of previous disk temperature modeling was provided to give context to the proposed numerical solutions. Further clarification regarding the evolutionary state of the  $\epsilon$  Aur system may result from the described analysis.

### 4. Acknowledgements

We appreciate the expert advice provided by Brian Kloppenborg while constructing this article. This work was supported in part by the bequest of William Herschel Womble in support of astronomy at the University of Denver, for which we are grateful.

### References

- Armitage, P. J. 2010, *Astrophysics of Planet Formation*, ed. P. J. Armitage, Cambridge Univ. Press, Cambridge.
- Carroll, S. M., Guinan, E. F., McCook, G. P., and Donahue, R. A. 1991, *Astrophys. J.*, **367**, 278.
- Dullemond, C. P. 2012, RADMC-3D: A new multi-purpose radiative transfer tool (<http://www.ita.uni-heidelberg.de/~dullemond/software/radmc-3d/>).
- Guinan, E. F., and Dewarf, L. E. 2002, in *Exotic Stars as Challenges to Evolution*, ed. C. A. Tout and W. van Hamme, ASP Conf. Ser., 279, Astron. Soc. Pacific, San Francisco, 121.
- Hartmann, L., Calvet, N., Gullbring, E., and D'Alessio, P. 1998, *Astrophys. J.*, **495**, 385.
- Hinkle, K. H., and Simon, T. 1987, *Astrophys. J.*, **315**, 296.
- Hoard, D. W., Howell, S. B., and Stencel, R. E. 2010, *Astrophys. J.*, **714**, 549.
- Hoard, D. W., Ladjal, D., Stencel, R. E., and Howell, S. B. 2012, *Astrophys. J., Lett. Ed.*, **748**, L28.
- Kloppenborg, B. K., Hemenway, P., Jensen, E., Osborn, W., and Stencel, R. 2011, *Bull. Amer. Astron. Soc.*, **43**, 230.05.
- Kloppenborg, B., et al. 2010, *Nature*, **464**, 870.
- Lambert, D. L., and Sawyer, S. R. 1986, *Publ. Astron. Soc. Pacific*, **98**, 389.
- Lin, D. N. C., and Papaloizou, J. 1985, in *Protostars and Planets II*, ed. D. C. Black and M. S. Matthews, Univ. Arizona Press, Tucson, 981.
- Lissauer, J. J., Wolk, S. J., Grith, C. A., and Backman, D. E. 1996, *Astrophys. J.*, **465**, 371.
- Muthumariappan, C., and Parthasarathy, M. 2012, *Mon. Not. Roy. Astron. Soc.*, **423**, 2075.
- Pequette, N., Stencel, R., and Whitney, B. 2011a, *Bull. Amer. Astron. Soc.*, **43**, 225.05.

- Pequette, N., Stencel, R., and Whitney, B. 2011b, private communication.
- Perryman, M. A. C., *et al.* 1997, *Astron. Astrophys.*, **323**, L49.
- Pollack, J. B., McKay, C. P., and Christoffersen, B. M. 1985, *Icarus*, **64**, 471.
- Robitaille, T. P. 2011, *Astron. Astrophys.*, **536**, A79.
- Saito, M., Kawabata, S., Saijo, K., and Sato, H. 1987, *Publ. Astron. Soc. Japan*, **39**, 135.
- Shakura, N. I., and Sunyaev, R. A. 1973, *Astron. Astrophys.*, **24**, 337.
- Sheffer, Y., and Lambert, D. L. 1999, *Publ. Astron. Soc. Pacific*, **111**, 829.
- Stefanik, R. P., Torres, G., Lovegrove, J., Pera, V. E., Latham, D. W., Zajac, J., and Mazeh, T. 2010, *Astron. J.*, **139**, 1254.
- Stencel, R. E., Creech-Eakman, M., Hart, A., Hopkins, J. L., Kloppenborg, B. K., and Mais, D. E. 2008, *Astrophys. J., Lett. Ed.*, **689**, L137.
- Stencel, R. E., *et al.* 2011, *Astron. J.*, **142**, 174.
- Takeuti, M. 1986a, *Astrophys. Space Sci.*, **120**, 1.
- Takeuti, M. 1986b, *Astrophys. Space Sci.*, **121**, 127.
- Takeuti, M. 2011, *Publ. Astron. Soc. Japan*, **63**, 325.

Table 1. Adopted  $\epsilon$  Aur system parameters using  $d = 625$  pc.

<i>Parameter</i>	<i>Value</i>	<i>Comments*</i>
<b>Primary Star</b>		
Temperature, $T_F$	7750 K	Based on F0 type and SED interferometric diameter (1) disk radial velocity (2)
Radius, $R_F$	$150 R_\odot$	
Mass, $M_F$	$3 M_\odot$	
<b>Secondary Star</b>		
Temperature, $T_B$	15000 K	Determined as B5V, from far-UV and He 10830 (3)
Radius, $R_B$	$4 R_\odot$	Based on B5V
Mass, $M_B$	$6 M_\odot$	Based on B5V
<b>Disk</b>		
Inner Radius, $R_{in}$	1 AU	Assumed
Outer Radius, $R_{out}$	3.8 AU	(4)
Observed Inclination	$89^\circ$	(4) and (5)
Disk Temperature	550–1150 K	Midnight to noon, relative to F star phase (6)
Observed Thickness/ $R_{out}$	0.08	(4)
Total number density at $R_{out}$	$1.6 \times 10^{12} \text{ cm}^{-3}$	obtained from CO lines (7)

\*References: (1) Stencel *et al.* (2008); (2) Lambert and Sawyer (1986); (3) Stencel *et al.* (2011); (4) Kloppenborg *et al.* (2010); (5) Hoard *et al.* (2010); (6) Hoard *et al.* (2012); (7) Hinkle and Simon (1987).

Table 2. Analytic disk equations, adopted from Armitage (2010).

Variable	Equation	Units	Equ. No.
viscosity	$\nu = \alpha c_s h$	$cm^2 s^{-1}$	1
sound speed	$c_s^2 = \frac{k_B T_c}{\mu m_p}$	$cm s^{-1}$	2
angular velocity	$\Omega^2 = GM_{\text{star}}/r_{\text{disk}}^3$	$s^{-1}$	3
density	$\rho = \frac{1}{\sqrt{2\pi}} \frac{\Sigma}{h}$	$g cm^{-3}$	4
scale height	$h = \frac{c_s}{\Omega}$	$cm$	5
mid-plane temperature	$T_c^4 = \frac{3}{4} \tau T_{\text{disk}}^4$	$K$	6
optical depth	$\tau = \frac{1}{2} \Sigma \kappa$		7
opacity	$\kappa = \kappa_0 T_c$	$cm^2 g^{-1}$	8
mass flow	$\nu \Sigma = \frac{\dot{M}}{3\pi}$	$g s^{-1}$	9
effective disk temperature	$T_{\text{disk}}^4 = \frac{9}{8} \frac{\nu}{\sigma} \Sigma \Omega^2 \left(1 - \sqrt{\frac{R_{\text{star}}}{r_{\text{disk}}}}\right)$	$K$	10
surface density	$\Sigma^4 = \frac{64\sigma}{27\kappa_0} \Omega \left(\frac{\mu m_p}{\alpha k_B}\right)^3 \left(\frac{\dot{M}}{3\pi}\right)^2 \left(1 - \sqrt{\frac{R_{\text{star}}}{r_{\text{disk}}}}\right)$	$g cm^{-2}$	11

Table 3. Analytical solutions using silicate dust.

$\kappa = \kappa_0 T_c$ , $\kappa_0 = 5 \times 10^{-3} cm^2 g^{-1} K^{-1}$ , $\alpha = 0.01$ , $\mu = 1.5$						
	$M_B = 6 M_\odot$			$M_B = 8 M_\odot$		
$\dot{M} [M_\odot/\text{yr}]$	$1.5 \times 10^{-5}$	$10^{-6}$	$10^{-7}$	$1.5 \times 10^{-5}$	$10^{-6}$	$10^{-7}$
$\Sigma [10^2 g cm^{-2}]$	67	17	5.5	70	18	57
$M_{\text{disk}} [10^{-3} M_\odot]$	34	8.9	3.5	41	9.2	2.9
$T_{\text{disk}} [K]$	520	270	150	560	290	160
$T_c [K]$	3600	920	290	4000	1000	330
$h [10^{12} cm]$	6.7	3.4	1.9	6.2	3.1	1.8
$h [AU]$	0.45	0.23	0.13	0.41	0.21	0.12
$3 h/R_{\text{out}}$	0.36	0.18	0.10	0.32	0.17	0.093
$2 h/R_{\text{out}}$	0.24	0.12	0.07	0.22	0.11	0.062
$h/R_{\text{out}}$	0.12	0.06	0.03	0.11	0.055	0.033
$n [10^{13} cm^{-3}]$	16	8.1	4.5	18	9.2	5.2

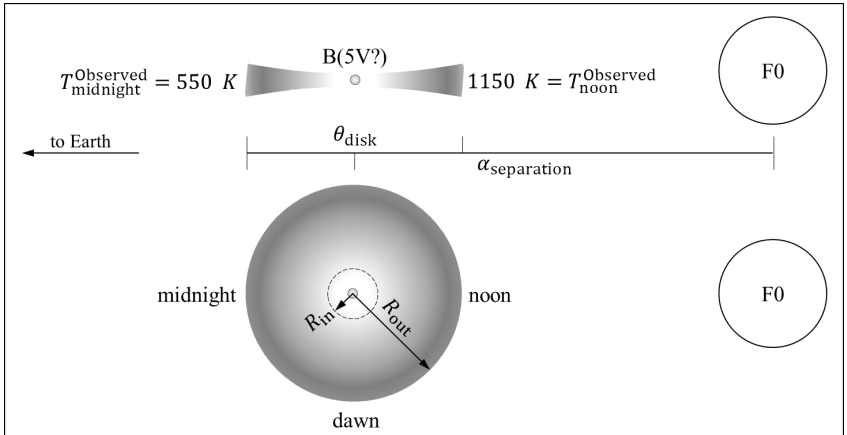


Figure 1. Side and top-view sketches (not-to-scale) of the  $\epsilon$  Aur system. Parameters coincide with values given in Table 1.

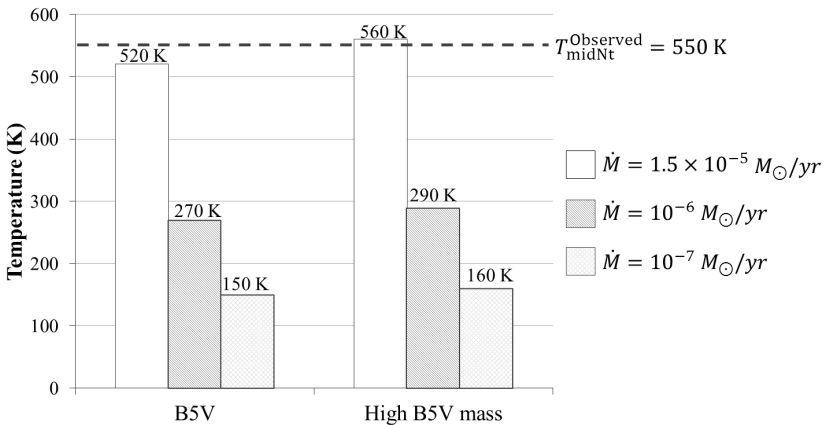


Figure 2. A chart displaying disk temperatures,  $T_{\text{disk}}$ , at the outer radius of the  $\epsilon$  Aur disk. These are results of an analytical study of the system. Two different central star masses were used in the calculations:  $M_B = 6 M_{\odot}$  and  $M_B = 8 M_{\odot}$ . The dotted line represents the known observed temperature,  $\langle T_{\text{midnight}}^{\text{Observed}} \rangle$ . Note that the only model to reach and exceed this value predicts a very high accreting rate of  $1.5 \times 10^{-5} M_{\odot}/\text{yr}$ , which is not physical for the  $\epsilon$  Aur system. Though the other accretion rates do not provide a matching temperature, they do compare to the minimum disk temperatures stated by Muthumariappan and Parthasarathy (2012) and Takeuti (2011).

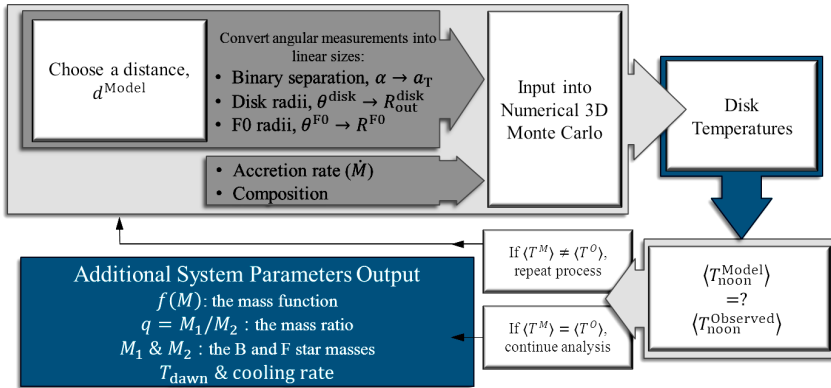


Figure 3. A schematic showing the process of solving for the distance to  $\epsilon$  Aur. Note that there are a few other input parameters besides just the binary separation. These include dust composition, dust molecular weight, and dust density distributions. See text for further information regarding analytical studies and numerical modeling, specifically with RADMC-3D.

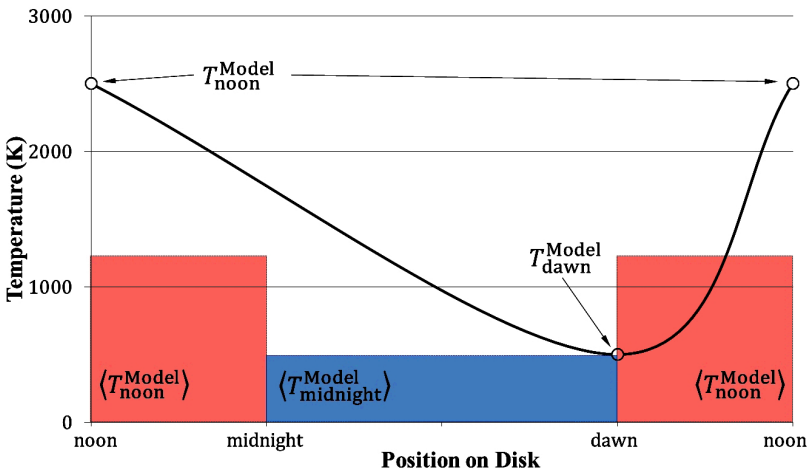


Figure 4. A plot describing the temperature distribution from a hypothetical numerical modeling reconstruction of  $\epsilon$  Aur, from RADMC-3D. The average “noon” and “midnight” temperatures were calculated by averaging the temperatures located at the outer edge of the disk, in the associated areas of the disk. The minimum and maximum temperatures associated with the numerical modeling are shown, as well as a hypothetical temperature gradient represented by the solid black line. Again, the line is not a fit to actual data: it is simply a graphical representation of a possible temperature distribution on the disk, outlined by the minimum and maximum temperatures. No accretional heating or disk rotation was used.